Materials Physics and Mechanics 47 (2021) 720-726
Research article

Received: August 2, 2021
Accepted: November 2, 2021

NON-CLASSICAL MODEL FOR DESCRIPTION OF THE DYNAMIC ELASTICITY MODULUS OF THE MATERIAL

M.A. Guzev[1,2], E.P. Riabokon[1]✉, M.S. Turbakov[1], V.V. Poplygin[1]

[1]Department of Oil and Gas Technologies, Perm National Research Polytechnic University, Perm 614990, Russia

[2]Institute for Applied Mathematics, Far Eastern Branch of the Russia n Academy of Sciences, Vladivostok 690041, Russia

✉ riabokon.evgenii@gmail.com

Abstract. A nonclassical gradient model of a continuous medium is proposed to describe the dispersion of Young's modulus of a rock sample observed under dynamic loading of the sample. The phenomenological parameters of the model are determined on the basis of an analysis of the results of experimental studies of the behavior of Young's modulus depending on the frequency and amplitude of the external loading.
Keywords: gradient model, dynamic modulus of elasticity, non-stationary load, material heterogeneity

***Acknowledgement**. The support of the Russian Science Foundation (Project No. 19-19-00408) is gratefully acknowledged.*

Citation: Guzev M.A., Riabokon E.P., Turbakov M.S., Poplygin V.V. Non-classical model for description of the dynamic elasticity modulus of the material // Materials Physics and Mechanics. 2021, V. 47. N. 5. P. 720-726. DOI: 10.18149/MPM.4752021_6.

1. Introduction

The materials used by engineers to create various structures are generally heterogeneous and their behavior during deformation is analyzed by researchers for a long time. The differentiation of the interests of specialists is associated, first of all, with the need to solve problems of different quality levels. In those levels, various mathematical models are required to describe the behavior of materials. Recently, non-classical models of a continuous medium [1-3] were actively used. Among the non-classical models, gradient models should be distinguished [4-8]. The gradient model was first proposed in [9]. Its modern application allowed to obtain solutions that clarify the description of macroscopic bodies, in which the stresses and deformations of the classical theory of elasticity have features. For example, the variants of gradient models developed in [10,11] allowed constructing non-singular solutions for describing materials with a structure. Gradient models are also used when considering non-classical effects of rock behavior [12,13]. It was shown in [14] that in the linear approximation the non-Euclidean and gradient models lead to the same result when describing the phenomenon of zonal disintegration in the material.

The dispersion of the elastic characteristics of the material under dynamic loading of sandstone samples is a non-classical effect of the rock behavior. Such an effect can be observed when using the rigs of split Hopkinson-Kolsky bar type [15,16], or on the rigs for

http://dx.doi.org/10.18149/MPM.4752021_6

uniaxial compression with an additionally installed oscillator [17]. In particular, in experimental works [18,19] on rigs with an oscillator, the dispersion of Young's modulus of a rock sample under dynamic loading was revealed. It should be noted that in the studies performed above a model describing the change in elastic characteristics under dynamic loading was not formulated. In [20], a corresponding model was proposed to describe the change in the dynamic component of Young's modulus of a rock sample under unsteady loading conditions. The authors proposed to consider the sample as a homogeneous material with a certain internal frequency. However, it is clear from the point of view of physics that the reason for the dispersion of Young's modulus is the heterogeneity of the rock structure. Therefore, the purpose of this work is to formulate a model that takes into account this heterogeneity to describe the behavior of rock under dynamic loading.

In Section 2, a gradient continuum model is used to describe the change in Young's modulus and to formulate dynamic relations taking into account the boundary conditions. In Section 3, a solution of the formulated equations is designed, on the basis of which phenomenological parameters are selected in Section 4.

2. Model formulation

According to the generalized theory given in [21], generalized stresses (including generalized strains) require to formulate constitutive relations. At the same time, in the one-dimensional case, the relationship between the stress σ and strain ε is established on the basis of the classical Hooke's law:

$$\sigma = E_{st}\varepsilon, \quad \varepsilon = \frac{\partial U}{\partial x}, \tag{1}$$

where E_{st} is Young's modulus; U is a displacement of sample particles. The experimental determination of Young's modulus in (1) is carried out under conditions of quasi-static loading of the material. The constitutive relations of the gradient model of a continuous medium can be obtained using the variational principle [22], which allows modifying the classical model. Then the equation of the state of the material is written in the form given below. Note that hereinafter the subscript x denotes the differentiation on a material coordinate:

$$\sigma = E_{st}\varepsilon - \gamma\varepsilon_{xx}. \tag{2}$$

Comparison of (2) with (1) shows that stress contains an additional contribution associated with taking into account the heterogeneity distribution of deformation in the material. Phenomenological parameter γ should be determined using data from experimental studies.

The dynamic Young's modulus is introduced according to the relation:

$$E_{dyn} = \frac{\sigma}{\varepsilon} = \frac{E_{st}\varepsilon - \gamma\varepsilon_{xx}}{\varepsilon} = E_{st} - \frac{\gamma}{\varepsilon}\varepsilon_{xx}. \tag{3}$$

In the experiments [23], a static load was applied to the upper end of the rock sample (sandstone) $F_{st} = 700$ N, which translated the sample into an elastic state. Then, a periodic (sinusoidal) load was applied to the upper end of the sample F_{dyn}. A change in the dynamic load led to a displacement of the upper-end surface of the sample, as a result of which the length of the sample changed from l_0 at F_{st} by the value Δl, reaching the maximum l_{max} at minimum dynamic load F_{dyn} and reaching the minimum l_{min} at maximum load F_{dyn} (Fig. 1a). Vertical displacement Δl of the upper-end surface of the sample was recorded by an eddy current probe (ECP). The study was carried out in the zone of linear behavior of the rock, which was previously determined in experiments on quasi-static compression (Fig. 1b). The recorded data on the displacement of the end surface of the sample were processed in the MATLAB package (Fig. 1c). Amplitude A of the dynamic load varied from 0 to 250 N, and the loading frequency ω was selected from 15 to 40 Hz. As a result of experiments with increasing ω. The dispersion of the dynamic component of Young's modulus was revealed for all amplitudes F_{dyn} (Fig. 1d). The studies were carried out on nine samples, for which 270 experiments were carried out. During the experiments, the stress in the sample for each loading cycle changed by the value $\Delta\sigma$.

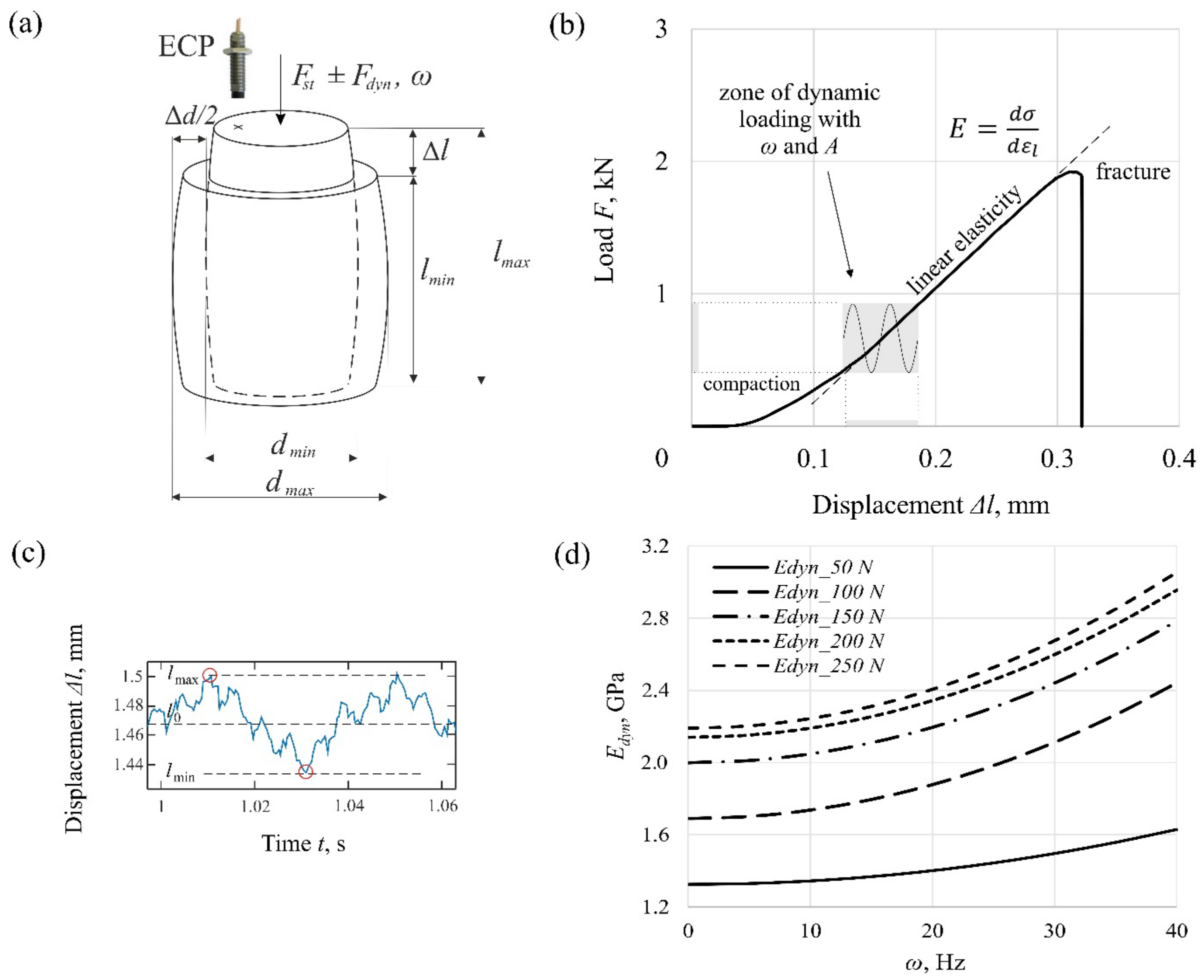

Fig. 1. Description of experiments on dynamic loading of rock samples: *a)* boundary shapes of the sample at maximum and minimum load (schematically); *b)* stress state of the sample; *c)* longitudinal displacement of the upper-end surface of the sample; *d)* dependence of the dynamic component of Young's modulus on the frequency of the applied periodic load

Thus, under the conditions of the experiment carried out, the value E_{dyn} (3) is calculated at the end of the sample, i.e.

$$E_{dyn} = E_{st} - \frac{\gamma\varepsilon_{xx}}{\varepsilon}\bigg|_{x=l_0}. \tag{4}$$

The momentum conservation law for a continuous medium has the form:

$$\rho_0 \frac{\partial^2 U}{\partial t^2} = \frac{\partial \sigma}{\partial x}. \tag{5}$$

Substituting (2) into (5), we obtain:

$$\rho_0 U_{tt} = E_{st}\varepsilon_x - \gamma\varepsilon_{xxx}. \tag{6}$$

Within the framework of the experiment carried out, the boundary condition for equation (6) at the upper end of the sample has the form:

$$\sigma|_{x=l_0} = E_{st}\varepsilon - \gamma\varepsilon_{xx}|_{x=l_0} = \frac{A}{S} sin\,\omega t. \tag{7}$$

At the lower end of the sample, there is no displacement of the particles of the medium, including the corresponding boundary condition for equation (6) is written in the form:

$$U|_{x=0} = 0. \tag{8}$$

3. Designing the solution

A solution for U in the form of a Fourier series looks like:

$$U = \alpha \sin \omega t \sin\lambda x + \sum_{k=1}^{\infty} \beta_k \sin(\Omega_k t + \varphi_k) \sin \lambda_k x, \quad (9)$$

wherein α, β_k are amplitude coefficients, φ_k is an initial phase, ω, λ and Ω_k, λ_k are internal model parameters. The structure of solution (9) is chosen so that it automatically satisfies condition (8). The relationship between the internal parameters is easy to obtain after substituting (9) in (6):

$$\omega^2 = \lambda^2 \upsilon_{st}^2 + \gamma \frac{\lambda^4}{\rho_0}, \Omega_k^2 = \lambda_k^2 \upsilon_{st}^2 + \gamma \frac{\lambda_k^4}{\rho_0}, \quad (10)$$

where the value $\upsilon_{st} = \sqrt{\frac{E_{st}}{\rho_0}}$ characterizes the velocity of propagation of an elastic wave in the material. Since the frequency ω is a given value, then the parameter λ is found from the first equation of the system (10):

$$\lambda^2 = \frac{-\upsilon_{st}^2 + \sqrt{\upsilon_{st}^4 + 4\frac{\gamma\omega^2}{\rho_0}}}{\frac{2\gamma}{\rho_0}}. \quad (11)$$

Selection of the corresponding sign at the root is given by the requirement that in the boundary case $\gamma \to 0$ solution for λ should be limited.

The fulfillment of the boundary condition (7) leads to the following restrictions:

$$\alpha(E_{st} + \lambda^2\gamma) \cos \lambda l_0 = \frac{A}{S}, \cos \lambda_k l_0 = 0.$$

From the first, we obtain a representation for the amplitude α:

$$\alpha = \frac{A/S}{(E_{st} + \gamma\lambda^2) \cos \lambda l_0}. \quad (12)$$

The second obtained limitation determines the set of oscillations (standing waves) in the sample that can form in it:

$$\lambda_k = \frac{\pi}{2} + \pi k ,$$

where k is a non-negative integer. From here and from (10), we can find the frequencies Ω_k.

In order to obtain the dependence of Young's modulus on the frequency of the dynamic load, we will use (4). This leads to the following model:

$$E_{dyn} = E_{st} + \gamma\lambda^2, \quad (13)$$

in which λ^2 is determined from (11). The experiment performed showed that the relative contribution of the dispersion term to the dynamic Young's modulus does not exceed 30%; therefore, (11) can be simplified by assuming $\lambda^2 \approx \frac{\omega^2}{\upsilon_{st}^2}$. Then (13) is reduced to the form:

$$E_{dyn} = E_{st} + \gamma \frac{\omega^2}{\upsilon_{st}^2}. \quad (14)$$

Since in dimension $[\omega] = \frac{1}{[time]}$, $[\upsilon_{st}] = \frac{[internal\ scale]}{[time]}$, then the dimension $[\gamma] = [internal\ scale]^2 [E_{st}]$. Thus, from the experiment, it is possible to estimate the value of the internal scale for which the model is used.

4. Selection of model parameters

Relations (10)-(13) contain an unknown parameter γ. To determine it, we will use formula (14) to process the experimental results

$$\gamma = \frac{\upsilon_{st}^2 (E_{dyn} - E_{st})}{\omega^2}. \quad (15)$$

Let us consider the velocity υ_{st} of the propagation of elastic vibrations in sandstone equal to $\upsilon_{st} = 2500$ m/s. Next, substitute the experimental data on the load frequency (varies from 0 to 40 Hz), dynamic and static Young's modulus for each dynamic load amplitude (varies from 0 to 250 N) (see Fig. 1d) into (15). As a result, we find that the parameter γ

belongs to the interval $\gamma \in [2437; 3375]$, Note that for each amplitude of the dynamic load there will be its own γ (Table 1).

Table 1. The heterogeneity parameter value for different loading amplitudes

Value of the parameter γ (N) for dynamic load amplitude A (N)					
0	50	100	150	200	250
0	1888	2757	3042	2592	3567

Let us consider an example of approximation of experimental data of the dynamic Young's modulus under dynamic loading of one of 9 rock samples. Perform an approximation for all of five amplitudes A of a dynamic load by the models (14), (13)+(11) and by the model (11) obtained in [20] and plot a graph for each load amplitude (Fig. 2). Note, that since there is no additional stress when the frequency of the dynamic load is equal to zero $\omega = 0$, in the graphs the value of E_{dyn} starts with a value of static Young's modulus E_{st}.

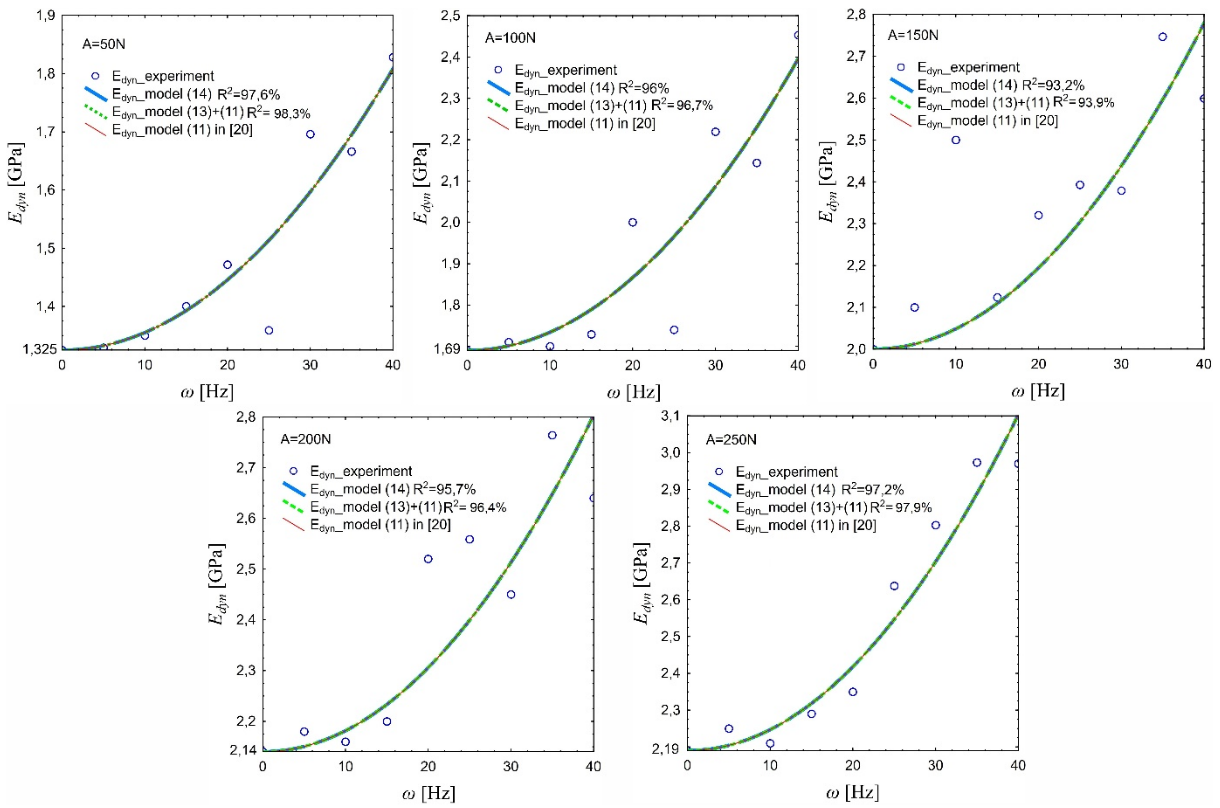

Fig. 2. Approximations of experimental data using models (14), (13)+(11) and the model (11) in [20]

It can be said from looking at Fig. 2 that the three approximations coincide. Since model (14) and model (11) from [20] both have quadratic relation, they indeed fit exactly. However, the approximation given by the model (13)+(11) has a higher level of matching to experimental data. The values of the dynamic Young's modulus E_{dyn} calculated using the model (14) in comparison with values calculated using a more precise model (13)+(11) are more accurate for 0.7%. Since it is precise and takes into account material heterogeneity, the model (13)+(11) is proposed for describing the material Young's modulus dispersion under dynamic loading.

5. Conclusion

A non-classical model of the change in Young's modulus of material under the action of a dynamic load is obtained. The model is based on the gradient theory of elasticity. The model contains an additive (parameter) responsible for the dispersion of the dynamic component of Young's modulus with increasing loading amplitude and load frequency. The additive represents the heterogeneity of the rock structure, which leads to the dispersion of the elastic characteristics of the heterogeneous material under dynamic loading.

References

[1] Forest S, Sievert R. Elastoviscoplastic constitutive frameworks for generalized continua. *Acta Mechanica.* 2003;160(1-2): 71-111.

[2] Smolin IY. On the application of the Cosserat model to the description of plastic deformation at the mesoscale. *Fizicheskaya Mezomekhanika*. 2005;3: 49-62.

[3] Bažant ZP, Jirásek M. Nonlocal integral formulations of plasticity and damage: Survey of progress. *Journal of Engineering Mechanics*. 2002;128(11): 1119-1149.

[4] Lurie SA, Kalamkarov AL, Solyaev YO, Volkov AV. Dilatation gradient elasticity theory. *European Journal of Mechanics, A/Solids*. 2021;88: 104258.

[5] Placidi L, Misra A, Barchiesi E. Simulation results for damage with evolving microstructure and growing strain gradient moduli. *Continuum Mechanics and Thermodynamics*. 2019;31(4): 1143-1163.

[6] Zhang G, Zheng C, Mi C, Gao XL. A microstructure-dependent Kirchhoff plate model based on a reformulated strain gradient elasticity theory. *Mechanics of Advanced Materials and Structures.* 2021. Available from: https://doi.org/10.1080/15376494.2020.1870054.

[7] Nazarenko L, Glüge R, Altenbach H. Positive definiteness in coupled strain gradient elasticity. *Continuum Mechanics and Thermodynamics.* 2021;33(3): 713-725.

[8] Sidhardh S, Ray MC. Element-free Galerkin model of nano-beams considering strain gradient elasticity. *Acta Mechanica.* 2018;229(7): 2765-2786.

[9] Mindlin RD. Micro-Structure in Linear Elasticity. *Archive for Rational Mechanics and Analysis.* 1964;16(1): 51-78.

[10] Aifantis EC. A note on Gradient Elasticity and Nonsingular Crack Fields. *Journal of the Mechanical Behavior of Materials.* 2012;20(4-5): 103-105.

[11] Parisis K, Konstantopoulos I, Aifantis EC. Nonsingular Solutions of GradEla Models for Dislocations: An Extension to Fractional GradEla. *Journal of Micromechanics and Molecular Physics*. 2018;3(3-4): 193-201.

[12] Guzev MA. Non-classical solutions of a continuum model for rock descriptions. *Journal of Rock Mechanics and Geotechnical Engineering.* 2014;6(3): 180-185.

[13] Qi CZ, Li KR, Bai JP, Chanyshev AI, Liu P. Strain Gradient Model of Zonal Disintegration of Rock Mass near Deep-Level Tunnels. *Journal of Mining Science.* 2017;53: 21-33.

[14] Lavrikov SV, Revuzhenko AF. Mathematical modeling of deformation of self-stress rock mass surrounding a tunnel. In: *Desiderata Geotechnica.* Springer; 2019. p.79-85.

[15] Lamzin DA, Bragov AM, Lomunov AK, Konstantinov AY, dell'Isola F. Analysis of the dynamic behavior of sand-lime and ceramic bricks. *Materials Physics and Mechanics.* 2019;42(6): 691-698.

[16] Petrov Y, Selyutina N. Dynamic behaviour of concrete and mortar at high strain rates. *Materials Physics and Mechanics.* 2013;18(2): 101-107.

[17] Borgomano JVM, Gallagher A, Sun C, Fortin J. An apparatus to measure elastic dispersion and attenuation using hydrostatic- And axial-stress oscillations under undrained conditions. *Review of Scientific Instruments.* 2020;91(3): 034502.

[18] Pimienta L, Fortin J, Guéguen Y. Bulk modulus dispersion and attenuation in sandstones. *Geophysics.* 2015;80(2): D111-D127.
[19] Lozovyi S, Bauer A. Static and dynamic stiffness measurements with Opalinus Clay. *Geophysical Prospecting.* 2019;67: 997-1019.
[20] Guzev M, Riabokon E, Turbakov M, Kozhevnikov E, Poplygin V. Modelling of the Dynamic Young's Modulus of a Sedimentary Rock Subjected to Nonstationary Loading. *Energies.* 2020;3: 646110.
[21] Vasiliev VV, Lurie SA. Nonlocal Solutions to Singular Problems of Mathematical Physics and Mechanics. *Mech. Solids.* 2018;53(2): S135-S144.
[22] Lomakin EV, Lurie SA, Rabinskiy LN, Solyaev YO. On the refined stress analysis in the applied elasticity problems accounting of gradient effects. *Doklady Physics.* 2019;489(6): 585-591.
[23] Guzev MA, Kozhevnikov EV, Turbakov MS, Riabokon EP, Poplygin VV. Experimental Studies of the Influence of Dynamic Loading on the Elastic Properties of Sandstone. *Energies.* 2020;13(23): 6195.

THE AUTHORS

Guzev M.A.
e-mail: guzev@iam.dvo.ru
ORCID: 0000-0001-9344-154X

Riabokon E.P.
e-mail: riabokon.evgenii@gmail.com
ORCID: 0000-0003-0555-3977

Turbakov M.S.
e-mail: msturbakov@gmail.com
ORCID: 0000-0002-9336-5847

Poplygin V.V.
e-mail: poplygin@bk.ru
ORCID: 0000-0003-2142-5246